Selective control of HOD photodissociation using low quanta O–D excitation and field optimized initial state (FOIST) based combination of states and colors

ARTICLE *in* CHEMICAL PHYSICS LETTERS · MARCH 2006

Impact Factor: 1.9 · DOI: 10.1016/j.cplett.2006.01.001

3 AUTHORS, INCLUDING:

Manabendra Sarma
Indian Institute of Technology Guwahati
22 PUBLICATIONS **66** CITATIONS
SEE PROFILE

Manoj Mishra
Cranfield University
83 PUBLICATIONS **447** CITATIONS
SEE PROFILE

Selective control of HOD photodissociation using low quanta O–D excitation and field optimized initial state (FOIST) based combination of states and colors

Manabendra Sarma [a,1], S. Adhikari [b], M.K. Mishra [a,*]

[a] Department of Chemistry, Indian Institute of Technology Bombay, Powai, Mumbai, Maharashtra 400 076, India
[b] Department of Chemistry, Indian Institute of Technology Guwahati, North Guwahati 781 039, India

Abstract

Selective Control of HOD photodissociation has been investigated using simple field profiles. Initial results indicate that preferential dissociation of O–H bond may be achieved from the ground vibrational state and that the O–D bond can be selectively dissociated using only the fundamental excitation in this mode. Dissociation from 2 quanta of excitation in the O–D mode produces 82.8% products with O–D bond dissociation. Preferential maximization of O–D dissociation vis-à-vis O–H bond may also be achieved from the ground vibrational state using a combination of two lasers with carrier frequencies 54920 cm^{-1} and 52203 cm^{-1}. The use of Field Optimized Initial STate (FOIST) based scheme to enhance selective control of HOD photodissociation provides additional $6-8\%$ H–O + D products compared to those obtained without FOIST.

1. Introduction

The use of high intensity ultra-short laser pulses for selective cleaving of bonds has attracted intense theoretical and experimental activity which has been presented extensively in many recent books and reviews [1–5], only a few of which are referred here for brevity. The HOD molecule has been a popular prototype for testing different approaches to selective cleaving of bonds [5–23] and continues to inspire new schemes for selective control of bond dissociation [17,20–23]. The H–OD and HO–D stretching frequencies in HOD are well separated [8,10,11,16,18] and provide for selective excitation of more or less pure O–H and O–D modes [5–8,10–16,18,19,22,24,25] in the ground electronic state. The first excited electronic state of HOD is purely repulsive with a saddle point barrier separating the H + O–D and H–O + D channels [26,27]. Excitation of an O–H or O–D bond mode provides preferential accumulation of the wave function in the H + O–D/H–O + D channels respectively [8,10,11,14,16,22]. Subjecting these excited bond modes to photolysis with UV frequencies which will deposit the stretched bond amplitude on the repulsive excited surface at an energy below the barrier height to prevent crossover to the other channel is an obvious recipe for rapid break up of the selected bond [7,8,10,12]. Vibrationally Mediated Photodissociation (VMP) of HOD utilizing an IR pulse for fundamental and overtone excitations of O–H or O–D mode followed by appropriate UV photolysis pulses have therefore provided some of the first experimental evidence for selective cleaving of bonds [9,12–15,19].

There is a kinematic bias in favor of larger amplitude motion in the O–H mode and preferential dissociation of the O–H bond (H–O–D → H + O–D) has been postulated [6–8,10,11,14,16,24] and demonstrated by many groups by subjecting the ground vibrational state and low/high overtone excitation of the O–H bond to appropriate photolysis pulses [9,12–15].

An analysis of the lobal topology of the excited O–D eigenmodes in conjunction with extent of the Franck Condon window for photolysis frequencies which will deposit them below the saddle point barrier on the repulsive excited surface has been used to predict and rationalise why 3 or more quanta of excitation in O–D mode is required for preferential dissociation of the O–D bond [8,10]. These predictions have been supported by the results obtained with Time Dependent Wave Packet (TDWP) calculations [8,10] and that, unlike in the case of H + O–D where one quantum of excitation in the O–H bond enhances its selective cleavage, there is no preferential dissociation of O–D bond with one quantum of excitation in the O–D mode has been supported by experimental results as well [15]. TDWP calculations [8,10] have postulated similar non preferential cleavage of the O–D bond even with two quanta of excitation in the O–D mode, and so far, at the lowest, 3 quanta of O–D excitation has been required to achieve preferential dissociation of the O–D bond [19]. Recently, photodissociation of the $|0,5\rangle$ state with 5 quanta of excitation in the O–D bond has been shown to provide remarkable preference for O–D dissociation which has been analysed in terms of lobal topology of the $|0,5\rangle$ state and its deposition below the excited state barrier for the photolysis frequency used in this experiment [22].

The rationalisations of non preferential dissociation of the O–D bond in HOD for low quanta O–D overtones are, however, based on calculations employing δ-function type pulses and semiclassical TDWP assumptions with implicit instantaneous transfer of population from the ground to the excited electronic state. As will be seen from our results, the transfer of population from the ground to excited state for reasonably wide UV pulses is non instantaneous and does not preserve the lobal topology of the wave function on the ground electronic state. The theoretical/experimental results postulating the need for 3 or more quanta of excitations in the O–D mode for preferential dissociation of the O–D bond in HOD therefore need further examination with fully quantal calculations.

Results presented in this letter indicate that H + O–D/H–O + D branching ratios in excess of 10 may be produced without any excitation of the O–H mode. Reversal of the kinematic bias in favor of the O–H bond dissociation to produce larger yield of H–O + D products however does require vibrational mediation and it is our purpose in this letter to investigate if considerable selectivity and yield in dissociation of the O–D bond may be achieved with easily realizable small quanta O–D excitations, and, if possible, from the ground vibrational state itself.

Use of appropriate IR lasers to achieve selective population of the desired $|m,n\rangle$ vibrational state with m and n quanta of excitation in O–H and O–D modes respectively has been demonstrated by several groups [18,19,22,25] and a mix of excited O–D modes has been used in Ref. [16]. We have therefore de-linked prior preparation of initial vibrational states from selective dissociation of the O–D bond and concentrated only on the mapping of the photolysis profile as a function of zero, one and two quanta of vibrational excitation in the O–D mode to try and provide an easier approach for selective dissociation of the O–D bond.

Furthermore, to exploit the dependence of photodissociation outcome on the initial vibrational state subjected to the photolysis pulse, we have been advocating the use of Field Optimized Initial STate (FOIST) scheme [28–30] which attempts to distribute the onus for selective control on both the field attributes and the molecular initial state subjected to the chosen photolysis pulse. The field attributes may be chosen for simplicity and chemical insight, and an optimal initial state is generated using FOIST. The FOIST scheme has been successfully applied for selective control of dissociation products in HI and IBr [28–30] and it is also our purpose in this letter to extend this approach to VMP of HOD to provide preliminary results from its application to selective cleaving of O–H and O–D bonds and to explore if we can supplant FOIST based mixing of vibrational states with much easier mixing of laser colors.

Brief systemic details and methodology are presented in the following section. In Section 3 we discuss our results. Summary of salient observations in Section 4 concludes this paper.

2. Method

The first and second excited electronic states of HOD are well separated and following earlier investigations [6–8,10,11,14,16,17,21,23,24], we too formulate the HOD dynamics considering only the ground and the first excited electronic state of this molecule. In the first absorption band ($\tilde{A}^1B_1 \leftarrow \tilde{X}^1A_1$) of HOD, excitation from the ground state ($\tilde{X}^1A_1$) to the repulsive first excited state ($\tilde{A}^1B_1$) induces a negligible change in the bending angle [6,7]. The bending mode is not active in the first absorption band [24], and hence the internal kinetic energy operator in terms of the conjugate momenta $\hat{p}_1$ and $\hat{p}_2$ associated with the O–H (r_1) and O–D (r_2) stretching co-ordinates respectively, is taken as [8,10,11,16,18,20,21]

$$\hat{T} = \frac{\hat{p}_1^2}{2\mu_1} + \frac{\hat{p}_2^2}{2\mu_2} + \frac{\hat{p}_1\hat{p}_2}{m_0}\cos\theta, \quad \text{where}$$
$$\hat{p}_j = \frac{\hbar}{\mathrm{i}}\frac{\partial}{\partial r_j}, \quad j = 1,2, \quad \mu_1 = \frac{m_H m_O}{(m_H + m_O)} \quad \mu_2 = \frac{m_D m_O}{(m_D + m_O)}. \tag{1}$$

and θ is the equilibrium bond angle (104.52°). The ground [8,10,31] and excited [26,27] Potential Energy Surface (PES), the transition dipole moment surface and the UV–molecule interaction Hamiltonian $H_{UV}(t)$ are same as those employed in other calculations on HOD [10,16]. The time evolution of the corresponding nuclear motion can then be performed using the time dependent Schrödinger equation,

$$i\hbar\frac{\partial}{\partial t}\begin{pmatrix}\Psi_g\\ \Psi_e\end{pmatrix} = \begin{pmatrix}\hat{H}_g & \hat{H}_{UV}(t)\\ \hat{H}_{UV}(t) & \hat{H}_e\end{pmatrix}\begin{pmatrix}\Psi_g\\ \Psi_e\end{pmatrix}, \tag{2}$$

where $\Psi_g = \Psi_g(r_1, r_2, t)$ and $\Psi_e = \Psi_e(r_1, r_2, t)$ are the wave functions associated with nuclear motion in the ground and first excited electronic states, respectively. $\hat{H}_g = \hat{T} + \hat{V}_g$ and $\hat{H}_e = \hat{T} + \hat{V}_e$ are the nuclear Hamiltonians for the two electronic states and $\hat{H}_{UV}$ couples as well as perturbs both the electronic states. We solve Eq. (2) with the initial condition that the ground state wave function Ψ_g is a single, field free, vibrational state of the HOD electronic ground state, and the excited state wave function $\Psi_e = 0$, at $t = 0$.

Vibrational eigenfunctions of the ground electronic state of the HOD molecule were obtained using the Fourier Grid Hamiltonian (FGH) method [32] modified for two dimensions [33]. The vibrational eigenfunctions ($|m,n\rangle$) of the ground electronic state and the corresponding eigenfrequencies compare quite well with those tabulated in ref. [16].

The propagation of the wavefunctions $\{\Psi_g(t), \Psi_e(t)\}$ has been performed using Eq. (2) where the effect of kinetic energy operator on the wavefunction is evaluated with a two dimensional Fast Fourier Transform (FFT) [34] and the time propagation is carried out using the Lanczos scheme [35]. The wave function is represented on a spatial grid spanning r_{O-H}/r_{O-D} bond lengths between 1 a_0 to 10 a_0 in 128 steps with $\Delta r_{O-H} = \Delta r_{O-D} \simeq 0.0703$ a_0 ($\simeq$0.0372 Å) and propagation of field effects under the influence of a generic Gaussian UV pulse of the form $E(t) = 0.09 * a(t)(\cos \omega t)$ where $a(t) = \exp[-\gamma(t - t_{UV})^2]$ with FWHM $= \sqrt{\frac{4 \ln 2}{\gamma}}$, is done in time steps of $\Delta t = 1$ a.u. of time $\simeq$0.0242 fs. Maximum field amplitude for the fields employed in our calculation is 0.46 GV/cm and maximum field intensity is 178 TW/cm^2. The extent of dissociation of O–H and O–D modes is determined from flux in the H + O–D and H–O + D channels calculated along asymptotic cuts at $r_{O-H} = 7.5$ a_0 and $r_{O-D} = 7.5$ a_0 in the H + O–D and H–O + D channels respectively. An absorbing ramp potential is placed immediately thereafter to avoid unphysical reflection from the edges.

In the FOIST scheme [28,30], the product yield is maximized through preparation of the initial wavefunction $|\Psi_g(r_1, r_2)\rangle$ as a superposition of the field free vibrational wavefunctions $\{\psi_m\}$ of the ground electronic state,

$$\Psi_g(0) = \sum_{m=0}^{M} C_m \psi_m, \tag{3}$$

The product yield in the desired channel is related to the time-integrated flux,

$$\begin{aligned} f &= \int_0^T \mathrm{d}t \langle \Psi(t) | \hat{j} | \Psi(t) \rangle \\ &= \int_0^T \mathrm{d}t \langle \Psi_g(0) | \hat{U}^\dagger(t,0) \hat{j} \hat{U}(t,0) | \Psi_g(0) \rangle = \langle \Psi_g(0) | \hat{F} | \Psi_g(0) \rangle \\ \text{with} \quad & \Psi(t) = \hat{U}(t,0)\Psi_g(0), \quad \hat{F} = \int_0^T \mathrm{d}t \hat{U}^\dagger(t,0) \hat{j} \hat{U}(t,0) \\ \text{and} \quad & \hat{j}_i = \frac{1}{2\mu_i} \left[\hat{p}_i \delta(r_i - r_i^d) + \delta(r_i - r_i^d) \hat{p}_i \right], \end{aligned} \tag{4}$$

where U is the time evolution operator, j_i is the flux operator in the ith channel and μ_i, $\hat{p}_i$ and r_i^d are the reduced mass, the momentum operator and a grid point in the asymptotic region of the ith channel denoted by reaction coordinate r_i, with H + O–D channel labelled as 1 and H–O + D channel as 2. The expressions for the total flux J in the H + O–D and H–O + D channels are then given by,

$$\begin{aligned} J_{H+O-D} = & \int_0^{r_{2d}} \int_0^T \Psi^*(r_1, r_2, t) \\ & \times (\hat{j}_1 + \frac{\mu_2 \cos\theta}{m_0} \hat{j}_2) \Psi(r_1, r_2, t) \mathrm{d}r_2 \mathrm{d}t \end{aligned} \tag{5}$$

$$\begin{aligned} J_{H-O+D} = & \int_0^{r_{1d}} \int_0^T \Psi^*(r_1, r_2, t) \\ & \times (\hat{j}_2 + \frac{\mu_1 \cos\theta}{m_0} \hat{j}_1) \Psi(r_1, r_2, t) \mathrm{d}r_1 \mathrm{d}t \end{aligned} \tag{6}$$

where the second operator in Eqs. (5) and (6) represents the effect of kinetic coupling between the O–H and O–D modes. The field dependence of H $(\vec{r}_1, \vec{r}_2, t)$ manifests itself through $U(t,0) \simeq e^{-iHt/\hbar}$ where $H = H_{molecule} + H_{UV}(t)$ and we can see that product yield $\langle \Psi_g(0) | \hat{F} | \Psi_g(0) \rangle$ in desired channel may be altered by altering the field or $\Psi_g(0)$. The time integrated flux operator $\hat{F}$ being hermitian, optimization of the channel and field specific flux functional $\langle \Psi_g(0) | \hat{F} | \Psi_g(0) \rangle$ with respect to the coefficients C_m employed in Eq. (3) leads to the Rayleigh–Ritz eigenvalue problem [28,29]

$$\mathbf{FC} = \mathbf{C}\mathbb{f} \tag{7}$$

where $\mathbb{f}$ is the diagonal matrix of eigenvalues of the time integrated flux matrix $\mathbf{F}$. The matrix elements of $\mathbf{F}$ in the ith channel are given by [29]

$$F_{kl}^i \approx \Delta t \sum_{n=0}^{N_t} \langle \psi_k(n\Delta t) | J_i | \psi_l(n\Delta t) \rangle \tag{8}$$

where $J_1 = (\hat{j}_1 + \frac{\mu_2 \cos\theta}{m_0} \hat{j}_2)$ and $J_2 = (\hat{j}_2 + \frac{\mu_1 \cos\theta}{m_0} \hat{j}_1)$.

We propagate the M initial states, included in the expansion manifold of Eq. (3) using spatial and temporal details presented earlier and calculate accumulated flux matrices (F_{kl}^i) both for the H + O–D and H–O + D dissociation channels. The accumulated $F_{kl}^{(H+O-D)}$ or $F_{kl}^{(H-O+D)}$ matrices are diagonalized and eigenvector (C_m^{max}) corresponding to the highest eigenvalue f_{max} indicates the maximum possible dissociation yield available for the field and the manifold of vibrational eigenstates chosen in that calculation. The C_m^{max} defines the initial wavefunction, $\Psi_g(0) = \sum_m C_m^{max} \psi_m$ which will provide ($f_{max} \times 100\%$) dissociation in the chosen channel (H + O–D for J_1 or H–O + D for J_2) for the field used in H_{UV}(t) and the expansion manifold of field free vibrational states (M) utilised in the calculation [29].

Selectivity and yield can also be influenced by supplementing or substituting the mixing of vibrational states by mixing additional colors (frequencies) [30] to the resonant carrier frequency with a single or multicolor field $E(t) = 0.09 * a(t) \sum_i \cos \omega_{UV}^i t$ where ω_{UV}^i are physically

motivated UV frequencies that induce transitions to same final state from different vibrational levels of the ground state and $a(t)$ represents the chosen field profile. The frequencies in this multicolor field are well separated so that mechanistic insights in terms of excitation from and dumping to specific vibrational levels may be attempted. Initital results from first application of these ideas to the selective control of bond dissociation in HOD are presented in the following section.

3. Results and discussion

Following more recent work on HOD [16,20] we too have utilised a gaussian UV pulse for photolysis except that temporal width of our pulse is larger (FWHM = 50 fs) to permit easy separation of frequencies involved in photodynamics. The simple gaussian pulse used by us and its power spectrum are depicted in Fig. 1. The frequency dependence of flux out of dissociative channels H + O–D ($J_{\mathrm{H+O\text{–}D}}$) and H–O + D ($J_{\mathrm{H\text{–}O+D}}$) of the HOD molecule using field profile of Fig. 1 and the frequency range covering the first absorption band for photolysis using $|0,0\rangle$, $|0,1\rangle$ and $|0,2\rangle$ as initial states are presented in Fig. 2.

It can be seen from Fig. 2 that with the ground vibrational state $|0,0\rangle$ as the initial state, due to the lower mass of H atom and the consequent ease for large amplitude vibrations in O–H vis-à-vis O–D, O–H dissociation dominates O–D dissociation as expected [6–8,10] and H + O–D flux predominates over the entire range of frequencies. However, unlike in the previous studies [12–15,20], a large variety in H + O–D/H–O + D product yield may be achieved without having to provide additional quanta of excitation in the O–H bond.

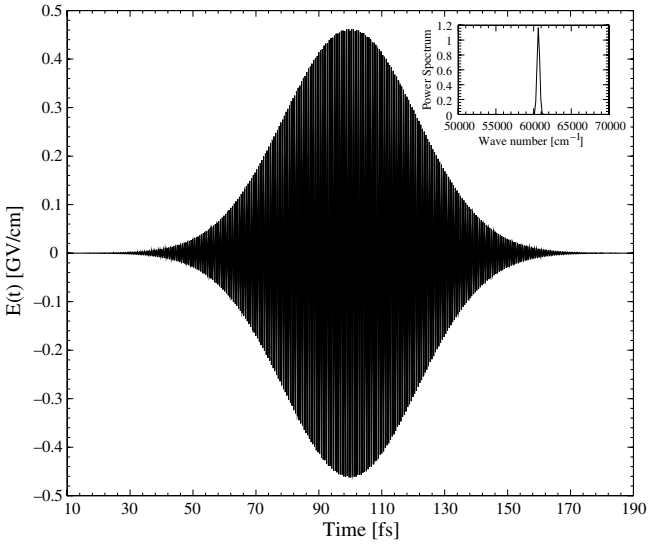

Fig. 1. UV laser pulse $E(t) = 0.09{*}a(t)(\cos\omega t)$. $a(t) = \exp[-\gamma(t - t_{\mathrm{UV}})^2]$ with FWHM $= \sqrt{\frac{4\ln 2}{\gamma}} = 50$ fs; $t_{\mathrm{UV}} = 100$ fs and $\omega = 60777$ cm^{-1}. Maximum field amplitude is 0.46 GV/cm and maximum field intensity is 178 TW/cm^2. The corresponding power spectrum is shown in the inset.

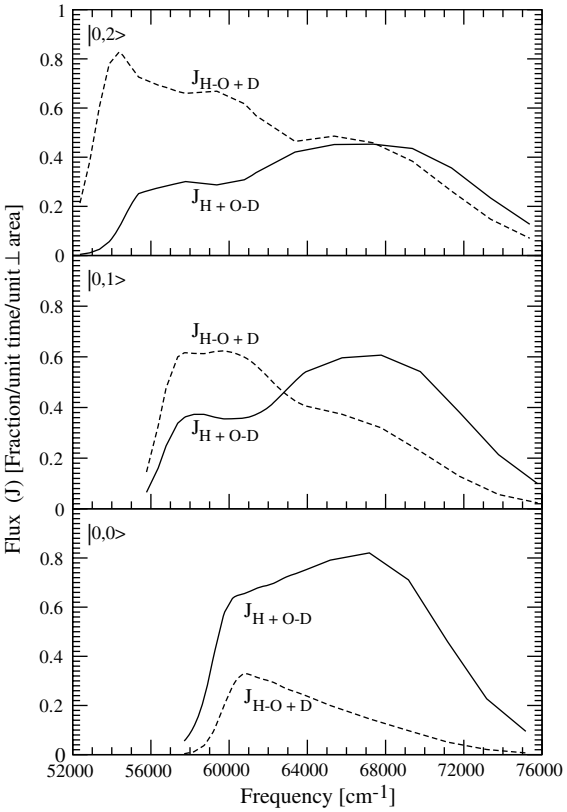

Fig. 2. Plot of flux vs. frequency for different initial states.

The $|0,1\rangle$ vibrational state with one quantum of excitation in the O–D mode is 2717 cm^{-1} higher than the $|0,0\rangle$ level and comes in resonance with the excited surface at lower UV frequencies. Hence, the dissociation in both the O–H and O–D modes picks up at frequencies lower than that for the $|0,0\rangle$ level. The $|0,1\rangle$ state has larger O–D stretch with the probability density peaking in the H–O + D channel. The natural preference for H + O–D dissociation is therefore reversed and the H–O + D flux is much more than the H + O–D flux in a broad range of frequencies. At higher frequencies the $|0,1\rangle$ begins to go off resonance with the excited surface and, the H + O–D flux predominates. Finally, at very high frequencies, the $|0,1\rangle$ level is completely off resonance vis-à-vis the repulsive excited surface and both the H + O–D and H–O + D flux values drop down to negligible levels.

Similarly, for $|0,2\rangle$ as the initial state with two quanta of vibrational excitations in the O–D mode, the O–D bond is

Table 1
Flux obtained using single initial state and laser pulse $E(t) = 0.09 * a(t)$ $(\cos\omega t)$ where $a(t) = \exp[-\gamma(t - t_{\mathrm{UV}})^2]$ with FWHM $= \sqrt{\frac{4\ln 2}{\gamma}} = 50$ fs

Initial state	Frequency ω (cm^{-1})	H + O–D flux (%)	H–O + D flux (%)
$\|0,0\rangle$	60777	65.5	32.9
$\|0,1\rangle$	59703	35.5	62.4
$\|0,2\rangle$	54372	11.5	82.8

Maximum field amplitude = 0.46 GV/cm and maximum field intensity is 178 TW/cm^2.

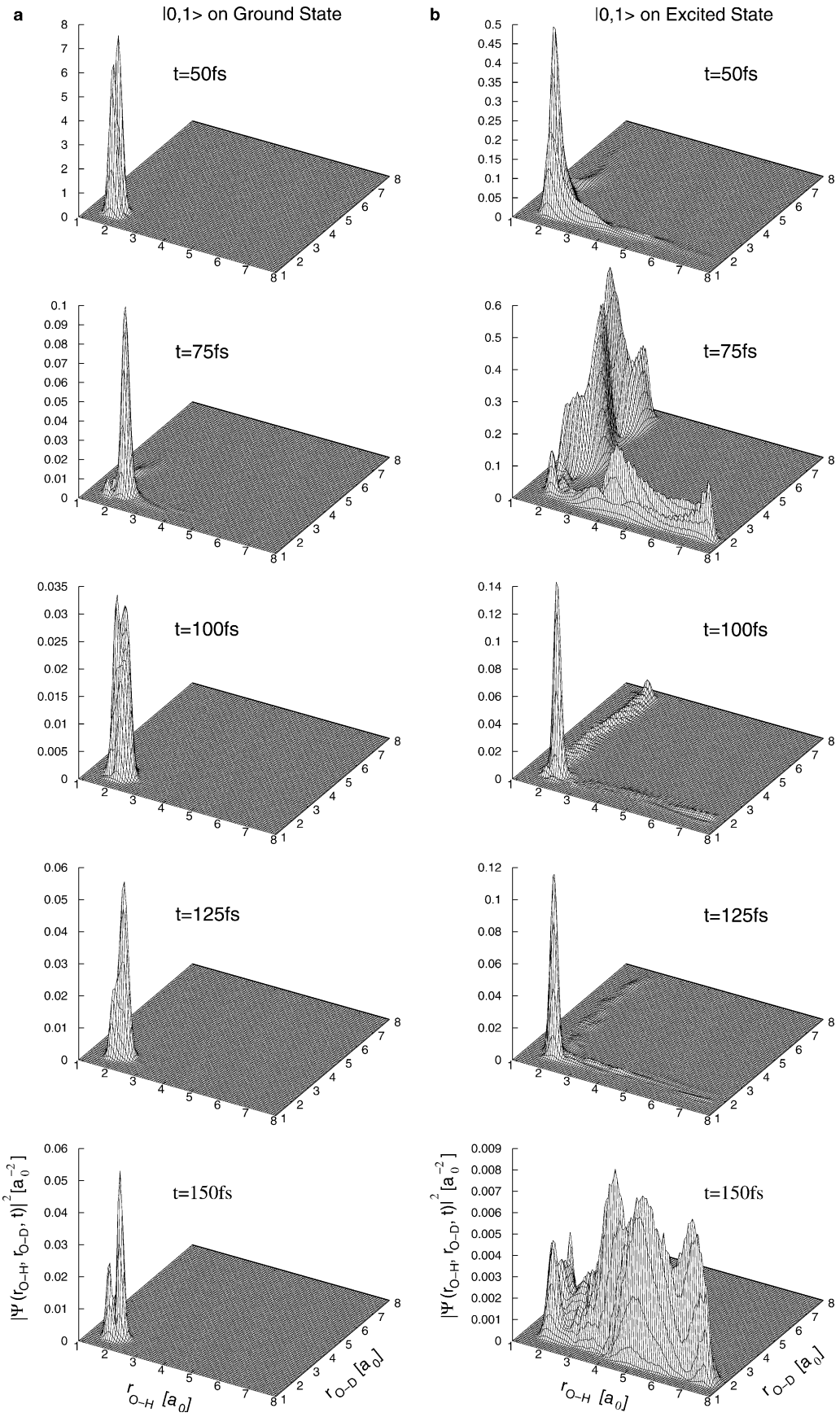

Fig. 3. Time evolution of $|0,1\rangle$ on: (a) ground, (b) first excited electronic state and (c) ground and excited state populations and accumulated H + O–D and H–O + D flux from $|0,1\rangle$ as the initial state under the influence of the field with same attributes as in Fig. 1 except with carrier frequency $\omega = 59\,703$ cm^{-1}.

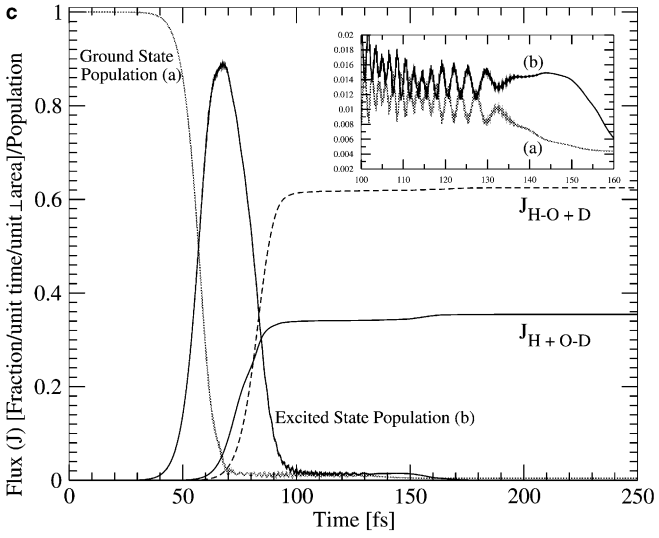

Fig. 3 (*continued*).

stretched much more and, as a result, H–O + D flux values increase to a maximum of about 83%. The $|0,2\rangle$ level being 5348 cm^{-1} above $|0,0\rangle$ comes in resonance with the repulsive excited state at lower frequencies. The dissociation begins at frequencies lower than even that for $|0,1\rangle$ and with much more pronounced bias in the probability distributions favoring H–O + D channel, the high dissociation in H–O + D mode is understandable.

To summarize, as shown in Fig. 2 $|0,0\rangle$ favors cleaving of O–H bond and gives maximum H–O + D flux of about 32.9% at 60777 cm^{-1}, $|0,1\rangle$ gives the maximum H–O + D flux of about 62.4% at 59703 cm^{-1} and for $|0,2\rangle$ it is the 54372 cm^{-1} pulse which gives maximum H–O + D flux of 82.8%. These values are collected in Table 1.

To understand mechanistic features which may assist in maximal selectivity and yield we have also examined the time evolution of $|\Psi_g(r_1,r_2,t)|^2$ and $|\Psi_e(r_1,r_2,t)|^2$ on the ground and excited PES. Results from the time evolution of $|0,1\rangle$ on ground and first excited electronic states, under the influence of UV field with the profile of Fig. 1 and 59703 cm^{-1} as the carrier frequency, are plotted in Fig. 3a and b. Fig. 4a and b trace the time evolution of $|0,2\rangle$ for the same pulse profile but with 54372 cm^{-1} as the carrier frequency. Both these frequencies were chosen for having provided maximum H–O + D flux for the corresponding initial states as noted previously.

A few snapshots from time evolution of the $|0,1\rangle$ state at 50, 75, 100, 125 and 150 fs on the ground and the repulsive excited surfaces are presented in Fig. 3a and b respectively. As can be seen from the time evolution plots on the ground surface (Fig. 3a), the nodal topology characteristic of the $|0,1\rangle$ state at 50 fs undergoes considerable distortions in the 75–150 fs plots and these signal an active manipulation of the spatial attributes of the $|0,1\rangle$ probability density profile through field induced mixing with other vibrational states, most probably by dumping from the excited electronic surface to different vibrational levels of the ground surface. This premise is buttressed by the population and flux plots of Fig. 3c where synchronised population transfer between the ground and excited states is clearly seen. We surmise that this change in the probability density profile on the ground surface leads to Franck Condon transitions to different regions of the excited surface and the initial bias of greater amplitude in the H + O–D channel at 50 fs (Fig. 3b and c) is altered in favor of greater flux in the H–O + D channel at 75, 100 and 125 fs (Fig. 3b) till the amplitude values are negligibly small and a surge in the H + O–D channel at 150 fs has little effect on the overall bias of much greater flux in the H–O + D channel and the final flux in the H–O + D channel (Fig. 3c and row 2, Table 1) is approximately twice as large as that in the H + O–D channel. Furthermore, the dynamic changes in the lobal topology of the $|0,1\rangle$ state in Fig. 3a show that appealing insights based on a fixed, static Frank Condon window may not always be correct.

Some snapshots from time evolution of the $|0,2\rangle$ at 50, 75, 100, 125 and 150 fs on the ground and excited surfaces are given in Fig. 4a and b respectively. It can be seen from the time evolution plots on the ground surface (Fig. 4a) that the nodal topology characteristic of the $|0,2\rangle$ state at 50 fs undergoes some distortion in the 75–150 fs plots but these are not as large as that for the $|0,1\rangle$ state. The spatial profiles on the excited state in Fig. 4b have much greater diversity and a marked flow in the H–O + D channel. The more dominant theme as seen from the population and flux profiles of Fig. 4c is the nearly similar magnitude of the amplitude on the ground and excited surfaces once major depletion has taken place between the 50–75 fs interval. As can be seen from Fig. 4c, there is near similarity of the total amplitude on the ground and excited surfaces, from 75 fs onwards with continuous exchange of field mediated probability flow between the two surfaces. Also due to the greater spatial bias of the $|0,2\rangle$ probability distribution towards the H–O + D channel, the H–O + D flux dominates H + O–D flux from the very beginning and as can be seen in Fig. 4c there is a surge of population in the excited state once the field is cut off at 150 fs. In the absence of field induced dumping, the depletion from the excited state stops around 150 fs which leads to large flow in the H–O + D channel at 150 fs and in Fig. 4b and c we do see a marked pick up in the H–O + D flux at this time.

We have also sampled H + O–D and H–O + D flux for a few different combination of colors/initial states and some prominent results are collected in Table 2. Tracking of time evolution of even a single vibrational state on both the surfaces is extremely demanding of computational resources and a very comprehensive investigation of FOIST based mixing of many vibrational states has therefore not been attempted in this initial investigation. For the frequencies sampled here, mixing of $|0,0\rangle + |0,1\rangle$ using a single color photolysis pulse (rows 1 & 2 of Table 2) does not offer any improvement over those obtained using only the $|0,1\rangle$ as the initial state. The use of a two color photolysis pulse in combination with FOIST based mixing of

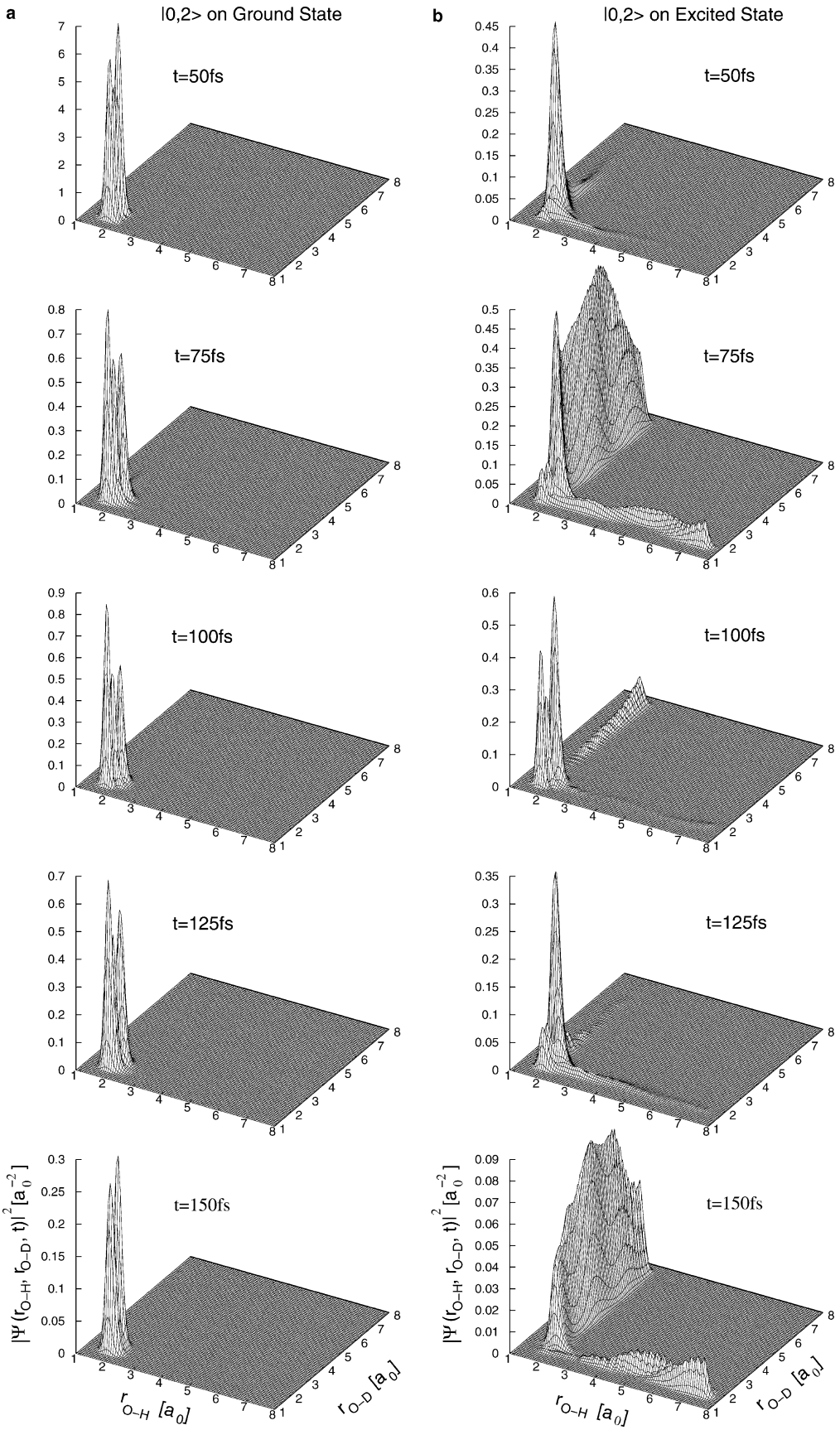

Fig. 4. Time evolution of $|0,2\rangle$ on: (a) ground, (b) first excited electronic state and (c) ground and excited state populations and accumulated H + O–D and H–O + D flux from $|0,2\rangle$ as the initial state under the influence of the field with same attributes as in Fig. 1 except with carrier frequency $\omega = 54372\ \mathrm{cm}^{-1}$.

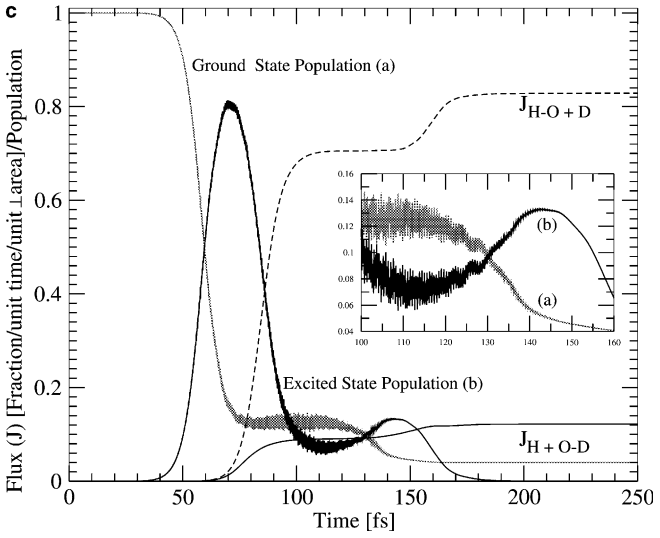

Fig. 4 (*continued*).

Table 2
Flux obtained using combination of color(s)/initial state(s), using laser pulse $E(t) = 0.09 * a(t) \sum_{i=1}^{2} \cos \omega_{UV}^{i} t$

Initial state(s)	Frequencies (cm^{-1})	H + O–D flux (%)	H–O + D flux (%)
$\|0,0\rangle + \|0,1\rangle$	59703	35.5	62.4
$\|0,0\rangle + \|0,1\rangle$	60777	35.9	59.9
$\|0,0\rangle + \|0,1\rangle$	60777 & 59703	31.8	66.2
$\|0,0\rangle + \|0,1\rangle$	60277 & 59703	30.3	67.9
$\|0,0\rangle$	54920 & 52203	26.4	47.2

$a(t)$ is same as that described for Table 1. ω_{UV}^{1} and ω_{UV}^{2} are carrier frequencies which provide maximum flux from $|0,0\rangle$ and $|0,1\rangle$ states selected from a large sampling of individual and two color combinations.

$|0,0\rangle$ & $|0,1\rangle$ (rows 3 & 4 of Table 2) however does offer $6-8\%$ more output in the H–O + D channel than that achieved without FOIST.

Finally, using $|0,0\rangle$ as the initial state and two lasers with frequencies 54920 and 52203 cm^{-1} where frequency difference between these lasers corresponds to the energy gap between the $|0,0\rangle$ and $|0,1\rangle$ vibrational levels, the H–O + D flux is much larger than the H + O–D flux. It is therefore a welcome surprise to report that the mixing of states may be supplanted by mixing of colors (Table 2, row 5) and for the two color laser setup, the H–O + D flux is approximately twice as the H + O–D flux even with the $|0,0\rangle$ as the initial state.

4. Concluding remarks

We have investigated the HOD photodissociation for selective O–D bond dissociation using simple field profiles. With ground vibrational state of the ground electronic state $|0,0\rangle$ as the initial state, the O–H dissociation is favored substantively over the O–D bond dissociation for a single color laser and preferential dissociation of the O–H bond may be achieved without additional excitation in the O–H mode.

Using $|0,1\rangle$ as the initial state with one quantum of excitation in the O–D mode, we find that favored dissociation of O–H bond is reversed for a large range of photolysis frequencies and H–O + D flux predominates over the H + O–D flux. Starting with $|0,2\rangle$ as the initial state with two quanta of excitation in the O–D mode, there is dominant dissociation of the O–D bond, for a large interval of frequencies.

A limited investigation of selective control of HOD photodissociation using the optimal superpositions selected by the Rayleigh–Ritz variational procedure for maximization of flux out of the desired channel for the chosen field indicates that further enhancement of $6-8\%$ in selective maximization of O–D dissociation may be possible through FOIST based selection of initial state. Furthermore, the mixing of vibrational states may be supplanted by mixing of colors and the kinematic bias in favor of O–H dissociation from the ground vibrational state $|0,0\rangle$ can be substantially reversed with a combination of two lasers with 54920 cm^{-1} and 52203 cm^{-1} as carrier frequencies providing approximately twice as much H–O + D as H + O–D.

In conclusion, our results provide a possibility for selective dissociation of O–D bond in HOD using only one or two quanta of excitation in the O–D mode. Furthermore, maximization of flux using appropriate combination of single/two color mixing of initial states using FOIST offers an additional alternative for laser assisted selective cleaving of O–H and O–D bonds in HOD.

It is our hope, that the results analysed here will attract requisite experimentation and will assist in reinvestigation of preferential dissociation of O–D bond in HOD using only one or two quanta of excitation in the O–D mode.

Acknowledgements

MKM acknowledges financial support from the Board of Research in Nuclear Sciences (Grant No. 2001/37/8/BRNS) of the Department of Atomic Energy, India. Manabendra Sarma acknowledges support from CSIR, India (SRF, F. No. 9/87(336)/2003-EMR-I). SA acknowledges Department of Science and Technology (DST), Government of India for partial financial support through the project No. SP/S1/H-53/01.

References

[1] M. Shapiro, P. Brumer, Principles of the Quantum Control of Molecular Processes, John Wiley and Sons, New York, 2003.
[2] S.A. Rice, M. Zhao, Optical Control of Molecular Dynamics, Wiley Interscience, New York, 2000.
[3] H. Rabitz, R.D.V. Riedle, M. Motzkus, K. Kompa, Science 288 (2000) 824.
[4] J. Manz, L. Wöste, Femtosecond Chemistry, VCH, Weinheim, 1995.
[5] F.F. Crim, Annu. Rev. Phys. Chem. 44 (1993) 397.
[6] V. Engel, R. Schinke, J. Chem. Phys. 88 (1988) 6831.
[7] J. Zhang, D.G. Imre, Chem. Phys. Lett. 149 (1988) 233.
[8] J. Zhang, D.G. Imre, J.H. Frederick, J. Phys. Chem. 93 (1989) 1840.
[9] N. Shafer, S. Satyapal, R. Bershon, J. Chem. Phys. 90 (1989) 6807.

[10] D.G. Imre, J. Zhang, Chem. Phys. 139 (1989) 89.
[11] B. Hartke, J. Manz, J. Mathis, Chem. Phys. 139 (1989) 123.
[12] R.L. Vander Wal, J.L. Scott, F.F. Crim, J. Chem. Phys. 92 (1990) 803.
[13] I. Bar, Y. Cohen, D. David, S. Rosenwaks, J.J. Valentini, J. Chem. Phys. 93 (1990) 2146.
[14] R.L. Vander Wal, J.L. Scott, F.F. Crim, K. Weide, R. Schinke, J. Chem. Phys. 94 (1991) 3548.
[15] I. Bar, Y. Cohen, D. David, T. Arusi - Parper, S. Rosenwaks, J.J. Valentini, J. Chem. Phys. 95 (1991) 3341.
[16] B. Amstrup, N.E. Henriksen, J. Chem. Phys. 97 (1992) 8285.
[17] N.E. Henriksen, B. Amstrup, Chem. Phys. Lett. 213 (1993) 65.
[18] J. Manz, G.K. Paramonov, J. Phys. Chem. 97 (1993) 12625.
[19] Y. Cohen, I. Bar, S. Rosenwaks, J. Chem. Phys. 102 (1995) 3612.
[20] N. Elghobashi, P. Krause, J. Manz, M. Oppel, Phys. Chem. Chem. Phys. 5 (2003) 4806.
[21] N.E. Henriksen, K.B. Møller, V. Engel, J. Chem. Phys. 122 (2005) 204320.
[22] H. Akagi, H. Fukazawa, K. Yokoyama, A. Yokoyama, J. Chem. Phys. 123 (2005) 184305.
[23] K.B. Møller, H.C. Westtoft, N.E. Henriksen, Chem. Phys. Lett. 419 (2005) 65.
[24] V. Engel, V. Staemmler, R.L. vander Wal, F.F. Crim, R.J. Sension, B. Hudson, P. Andresen, S. Hennig, K. Weide, R. Schinke, J. Phys. Chem. 96 (1992) 3201.
[25] M.V. Korolkov, J. Manz, G.K. Paramonov, Adv. Chem. Phys. 101 (1997) 327.
[26] V. Staemmler, A. Palma, Chem. Phys. 93 (1985) 63.
[27] V. Engel, R. Schinke, V. Staemmler, J. Chem. Phys. 88 (1988) 129.
[28] K. Vandana, M.K. Mishra, J. Chem. Phys. 110 (1999) 5140.
[29] K. Vandana, M.K. Mishra, Adv. Quant. Chem. 35 (1999) 261.
[30] K. Vandana, M.K. Mishra, J. Chem. Phys. 113 (2000) 2336.
[31] J.R. Reimers, R.O. Watts, Mol. Phys. 52 (1984) 357.
[32] C.C. Marston, G.G. Balint - Kurti, J. Chem. Phys. 91 (1989) 3571.
[33] P. Dutta, S. Adhikari, S.P. Bhattacharyya, Chem. Phys. Lett. 212 (1993) 677.
[34] D. Kosloff, R. Kosloff, J. Comp. Phys. 52 (1983) 35.
[35] C. Leforestier, R.H. Bisseling, C. Cerjan, M.D. Feit, R. Friesner, A. Guldberg, A. Hammerich, G. Jolicard, W. Karrlein, H.D. Meyer, N. Lipkin, O. Roncero, R. Kosloff, J. Comp. Phys. 94 (1991) 59.